BIOCELL
2022 46(1): 285-296

Tech Science Press

Differential metabolome landscape of *Kadsura coccinea* fruit tissues and potential valorization of the peel and seed tissues

Jianfei GAO[1]; Kangning XIONG[2,*]; Weijie LI[1]; Wei ZHOU[3]

[1] Institute of Mountain Resources, Guizhou Academy of Sciences, Guiyang, 550001, China
[2] School of Karst Science, Guizhou Normal University, State Engineering Technology Institute for Karst Desertfication Control of China, Guiyang, 550001, China
[3] Guizhou Industry Polytechnic College, Guiyang, 550008, China

Key words: *Kadsura coccinea*, Widely-targeted metabolomics, Alkaloids, Lignans, Flavonoids, Fruit, Biowaste valorization

Abstract: *Kadsura coccinea* (Lem.) is a woody wine plant with a peculiar fruit enriched in important health-promoting compounds. The non-editable part of the fruit, i.e., the seed and peel, represents more than 60% of the fruit and is considered a biowaste. This significantly restricts the development of the *K. coccinea* fruit industry. Clarifying the metabolic components of the different fruit parts can help to improve the utilization rate and valorization of *K. coccinea*. Herein, we evaluated *K. coccinea* fruit peel, pulp, and seed using widely-targeted metabolomics and quantified a set of 736 bioactive compounds from 11 major metabolite classes. The most prominent metabolite classes included lipids, amino acids, flavonoids, and lignans. Furthermore, our results emphasized a significant accumulation of flavonoids in pulp tissues, while alkaloids and lignans were abundant in peel and seed tissues, respectively. A total of 183 metabolites were differentially accumulated among the three tissues. Procyanidin C2, rutinoside, 2-hydroxyoleanolic acid, 5-hydroxymethyluracil, nootkatol, isoquercitrin, isohyperoside, quercetin-7-O-glucoside, hyperin, and rutin showed elevated accumulation in the peel. In the seed, kadsuralignan G, kadcoccilactone A, kadsuralignan H, lysoPE 20:5, iso-schisandrin ethyl alcohol, and kadangustin were significantly enriched. Our results highlight the diverse metabolome composition of *K. coccinea* fruit parts, which can be further exploited for its valorization in various industries.

Introduction

Black tiger (*Kadsura coccinea* (Lem.)) is a perennial evergreen climbing woody vine indigenous to Southwest China (Sun *et al.*, 2009) and widely distributed in Guizhou, Guangxi, Yunnan, Guangdong, and Sichuan (Sritalahareuthai *et al.*, 2020a). The mature black tiger fruit is usually consumed as fresh fruit. However, the edible portion of the fruit is only 30–40%, which is relatively lower compared to popular fruits. The high proportion of skin and seed weights of black tiger fruit is one of the main reasons for its low commercial value. Bioactive compounds present in different plant parts are an excellent source for potential valorization and value addition of the fruit plants. Previous studies emphasized valorization of plant biowaste by utilizing a broad spectrum of bioactive compounds present in plant parts generally considered biowaste. Deng *et al.* (2020) and Wang *et al.* (2020a), in their studies on banana pseudo-stem and longan fruit parts (skin and seed), respectively, demonstrated the potential valorization of biowaste by exploiting the metabolome and identified several compounds with nutraceutical properties. Hence, investigating the metabolome composition of black tiger fruit parts could open a new avenue towards a better valorization of the fruit and the development of the industry.

Kadsura genus, with extensive uses in traditional medicine (Yang *et al.*, 2020), is known as an abundant source of lignans and terpenoids (Yang *et al.*, 2019b), exhibiting several biological functions with beneficial properties, i.e., anti-tumor (Liu *et al.*, 2014), cytotoxic (Hu *et al.*, 2016), anti-HIV (Gao *et al.*, 2008b), antioxidative (Cao *et al.*, 2019), anti-hepatitis (Kuo *et al.*, 2005) and hepatoprotective effects (Liu *et al.*, 2018a). *K. coccinea* is an important raw material for traditional Chinese medicine. Different plant parts of *K. coccinea*, including rhizomes, bark, stem, and fruit, have been widely used as raw ingredients for the formulation of traditional Chinese medicine (Li *et al.*, 2006; Li *et al.*, 2007; Yang *et al.*, 2020) and subsequently utilized for the treatment of ulcer, acute gastroenteritis, rheumatoid arthritis, bruise, pain, and

*Address correspondence to: Kangning Xiong, xiongkn@163.com
Received: 22 February 2021; Accepted: 02 April 2021

Doi: 10.32604/biocell.2021.016253

dysmenorrhea (Wang *et al.*, 2020b). However, there is a lack of studies concerning the different parts of the fruit and their potential utilization as dietary or medicinal sources.

The fruit of the black tiger, with its peculiar shape, appearance, bright color, and unique flavor, possesses high health and medicinal values (Hao *et al.*, 2014; Sritalahareuthai *et al.*, 2020a; Sun *et al.*, 2009). Black tiger fruit is highly nutritive, with a higher vitamin C content as compared to common fruits such as apple, cherry, grape, Kiwi, litchi, and strawberry (El-Ishaq and Obirinakem, 2015). In our preliminary study, we found some biological activities of black tiger fruit peel and seed extracts. If the metabolic components of black tiger fruit parts are elucidated, the value of the non-edible part can be further explored with potential utilization in the food and pharmaceutical industries. Therefore, this study was designed to aim at exploring the differential metabolome of fruit parts, including peel, pulp, and the seed of black tiger fruit, based on the widely-targeted metabolomics approach.

Materials and Methods

Plant material

The black tiger plants, locally known as 'HeiLaohu', used in the experiment, resulted from 6 years of artificial cultivation. They were planted in an 80% plastic canopy with a sunshade net. The experiment was conducted in Xiaba, Wudang District, Guiyang, China, with regular management practices. Randomly selected fruits were picked during the maturation season in October 2020. Each selected fruit was rinsed with tap water, placed on a small plate, and cut with a scalpel. The peel and the pulp parts were slowly stripped out and collected separately into 10 mL centrifuge tubes. The seeds were rubbed in an emery cloth for seed tissue sampling to remove the flesh and then put into a 10 mL centrifuge tube. Three biological repeats for each sample from the peel, pulp, and seed were collected from three different fruits. Samples were stored at −80°C for further use.

Sample preparation

The samples were prepared according to Deng *et al.* (2020). The three groups of samples, cryopreserved, were freeze-dried in a vacuum using lyophilizer (Scientz-100F) and ground to powder. A 100 mg powder was accurately weighed and thawed in 1.2 mL 70% methanol extract (Shanghai Aladdin Bio-Chem Technology Co., Ltd., Shanghai, China). The samples were centrifuged every 30 min for 30 s, a total of six times. The samples were placed in a refrigerator at 4°C overnight. After centrifugation, at 12000 rpm for 10 min, the supernatant was absorbed, and later, samples were filtered with 0.22 μm-pore size (ALWSCI Technologies Zhejiang, China) and stored in injection bottles for further analysis.

UPLC-MS/MS analysis

The ultraperformance liquid chromatography-tandem mass spectrometry (UPLC-MS/MS performed by Metware, Wuhan, China) was used as a widely targeted metabolomics approach to detect and quantify the metabolome in the three black tiger fruit tissues including, peel, pulp, and seed. The sample extracts were analyzed using a UPLC-ESI-MS/MS system (UPLC, SHIMADZU NexeraX2, www.shimadzu.com.cn/; MS, Applied Biosystems 4500 Q TRAP, www.appliedbiosystems.com.cn/). The analytical conditions were as follows, UPLC: column, Agilent SB-C18 (1.8 μm, 2.1 mm × 100 mm); The mobile phase consisted of solvent A and solvent B. Solvent A consisted of pure water with formic acid (0.1%), and solvent B consisted acetonitrile with formic acid (0.1%) (Shanghai Aladdin Bio-Chem Technology Co., Ltd., Shanghai, China). The gradient program was used to measure the samples with a starting point of 95% A, 5% B. After 9 min, the linear gradient was changed to 5% A, 95% B for 1 min. Later, at 1.10 min, the gradient was adjusted back to 95% A, 5.0% B for 2.9 min. The flow velocity was kept constant during the whole gradient process as 0.35 mL/min. Moreover, the temperature was also kept constant at 40°C, while the injection volume was 4 μL.

AB4500 Q TRAP UPLC/MS/MS (triple quadrupole-linear ion trap mass spectrometer) system was utilized to perform ESI-triple quadrupole-linear ion trap (ESI-Q TRAP-MS/MS). The system was equipped with an ESI turbo Ion spray interface. Analyst 1.6.3 was used to control the system (Xu *et al.*, 2020).

ESI-Q TRAP-MS/MS

For ESI-triple quadrupole-linear ion trap (QTRAP)-MS, LIT, and triple quadrupole (QQQ) scans were acquired on a triple quadrupole-linear ion trap mass spectrometer (Q TRAP), AB4500 Q TRAP UPLC/MS/MS System, equipped with an ESI Turbo Ion-Spray interface, operating in positive and negative ion mode and controlled by Analyst 1.6.3 software (AB Sciex). The ESI source operation parameters were kept as explained by Chen *et al.* (2013).

Quality control and data analysis

To confirm the reliability of metabolome data sets, quality control was performed, as previously described by Fiehn *et al.* (2008). Extracted samples were mixed and inserted into every sample, and changes were monitored (Yang *et al.*, 2019a). Data sets with the intensity of the metabolites from the three samples were uploaded to the Analyst 1.6.3 software (AB SCIEX, Ontario, ON, Canada) for descriptive statistical analyses (Dossa *et al.*, 2020). Unsupervised principal component analysis (PCA) was performed by statistics function prcomp within R (www.r-project.org).

Differential metabolites

Significantly differentially accumulated metabolites between the fruit tissues were estimated by exploring the variable importance in projection (VIP) values greater than 1 with Log_2 fold change (FC) also greater than 1. Before Orthogonal Projections to Latent Structures-Discriminant Analysis (OPLS-DA), data was transformed as log_2FC, and mean centering was also performed. OPLS-DA results were used for the extraction of VIP values using R software with MetaboAnalystR package. Subsequently, 200 permutations were performed for each sample.

Results

Metabolic landscape in black tiger fruit parts

The UPLC-MS/MS technique was employed for metabolic profiling of black tiger fruit parts viz., peel, pulp, and seed

(Fig. 1). Repeatability of metabolites detection was ensured by observing the accuracy of the instrument using quality control, as previously explained by Fiehn *et al.* (2008). We observed overlapped peaks of the total ion current in different quality control samples (Fig. 2a). The results depicted overlapped and consistent peaks for ion-intensity peaks (showed on the y-axis) and retention time. Furthermore, the analysis showed stable peaks for identical samples for different time intervals.

Principal component analysis (PCA) was executed to evaluate the structure of the data. The PCA plot showed the distribution of three groups based on metabolite ion intensity in specific tissues (Fig. 2b). We observed a close grouping of biological replicates in each tissue, while all three tissues viz., peel, pulp, and seed were in separate groups, suggesting that high-quality metabolome data was obtained. Metabolome variance explained by the first two PCs was accumulatively high (90.34%).

After a quality check, we identified 736 metabolites, grouped into 11 major classes and 35 sub-classes (Fig. 3 and Tab. S1). The classification was based on the structural configuration of the identified metabolites. Of the 736 metabolites, lipids (17.66%) showed the highest proportion, followed by phenolic acids and derivatives (16.17%), amino acids and derivatives (13.18%), flavonoids (11.55%), organic acids (10.87%), others (10.05%), nucleotides and derivatives (6.52%), lignans and coumarins (5.57%), terpenoids (4.35%), alkaloids (2.17%), and tannins (1.90%) (Fig. 3). Complete information about the set of identified metabolites, including molecular weights (Da), compound formula, ionization, compounds, classes, and KEGG pathways, are listed in Tab. S1. The concentration (ion intensity) of the identified metabolites has been presented as a heatmap (Fig. 4), depicting their differential accumulation across the three tissues. Flavonoids, phenolic acids, terpenoids, and tannins showed relatively higher concentrations in the peel than in the pulp and seed. However, lignans and coumarins showed the highest accumulation in the seed.

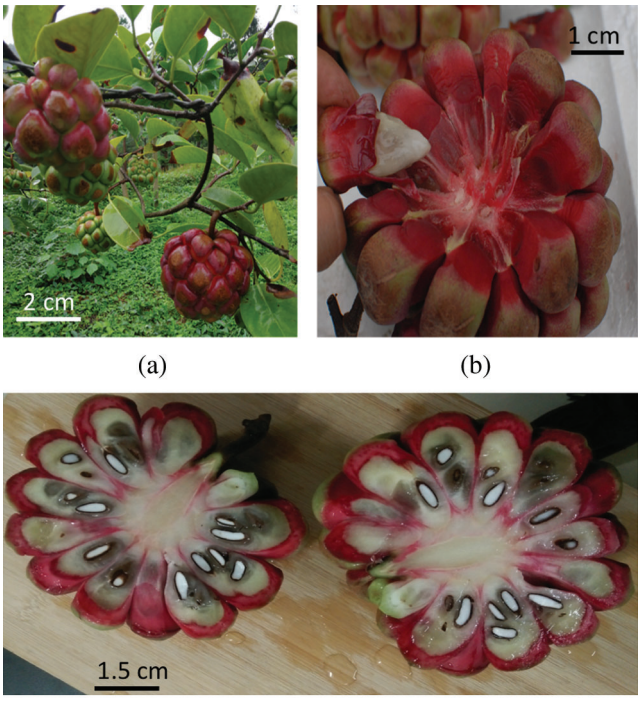

FIGURE 1. A pictorial description of black tiger fruit (*Kadsura coccinea* (Lem.)).
(a–b) Black tiger fruit. (c) Cross section of black tiger fruit.

Differential metabolic landscape

In order to understand the metabolic properties of the three fruit tissues, we identified the differentially accumulated metabolites (DAMs) between the tissues. In KF *vs.* KP, we obtained 299 DAMs (Tab. S2), 492 DAMs in KF *vs.* KD (Tab. S3), and 533 DAMs in KP *vs.* KD (Tab. S4). We further identified 183 conserved DAMs between the three groups (Fig. 5 and Tab. S5). These conserved DAMs can be categorized into ten major metabolites classes viz., alkaloids, amino acids, flavonoids, lignans and coumarins, lipids, nucleotides and derivatives, organic acids, phenolic acids, tannins, and terpenoids. The differential accumulation profile of these conserved metabolites has been illustrated in Fig. S2, indicating an up-accumulation of 114 DAMs in the peel (Tab. S5). While 37 and 38 DAMs were up-accumulated in the seed and pulp, respectively. This indicates that the peel contains more bioactive compounds even than the pulp. The most noticeable DAMs between pulp and peel were procyanidin C2, quercetin-3-O-(2”-O-arabinosyl) rutinoside, 2-hydroxyoleanolic acid, 5-hydroxymethyluracil, nootkatol, quercetin-3-O-glucoside (isoquercitrin), isohyperoside, quercetin-7-O-glucoside, quercetin-3-O-galactoside (hyperin), and quercetin-3-O-rutinoside (rutin).

Further, we explored the metabolome of black tiger fruit by comparing differential accumulation between pairs of tissues. Comparison of pulp and peel (KF *vs.* KP) yielded 299 DAMs (Tab. S2). The accumulation profile of these DAMs has been presented as a heatmap (Fig. 6a) with corresponding classes. A total of 168 DAMs were found with an up-accumulation pattern in the peel, while 131 DAMs were up-accumulated in the pulp. The top 10 DAMs up-accumulated in peel were flavonoids: delphinidin-3-O-glucoside (mirtillin), isorhamnetin-3-O-glucoside, myricetin-3-O-glucoside, quercetin-3-O-(2”-O-rhamnosyl) rutinoside, quercetin-3-O-rutinoside-7-O-rhamnoside, taxifolin-3’-O-glucoside, delphinidin-3-O-(2”-O-glucosyl) rutinoside, quercetin-3-O-sambubioside, eriodictyol-3’-O-glucoside, and tannins: procyanidin C2 (Fig. 6b). In contrast, the pulp showed a high accumulation of L-alanine, kadangustin I, kadangustin G, eicosadienoic acid, acetylepigomisin R, pregomisin, kadangustin F, kadusurain C, kadsuralignan J, and N-α-acetyl-L-ornithine (Fig. 6b).

Similarly, a comparison of pulp and seed resulted in the identification of 492 DAMs, with 115 metabolites up-accumulated in the seed while 377 were up-accumulated in the pulp (Fig. 7a and Tab. S3). Kadsuralignan G, kadcoccilactone A, kadsuralignan H, lysoPE 20:5, iso-schisandrin ethyl alcohol, kadangustin H, gomisin G, schisandrol B, maslinic acid, and plaunol E showed strong accumulation in the seed (Fig. 7b). While, p-coumaric acid,

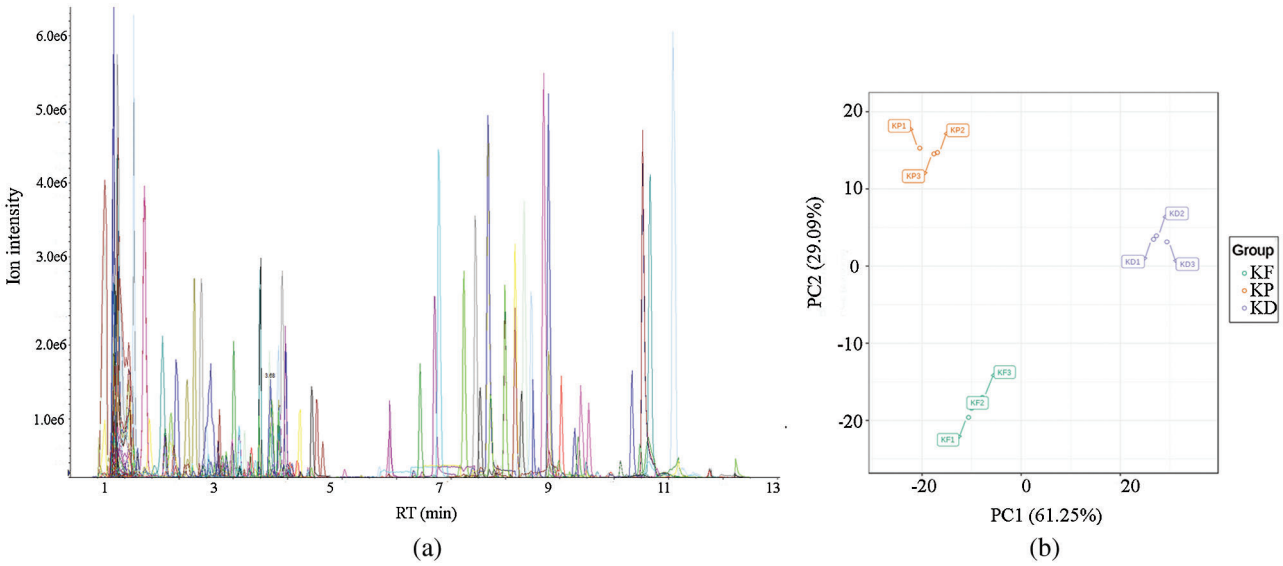

FIGURE 2. Quality control analysis for consistent metabolites measurements.
(a) The vertical axis represents the intensity of the ion current (cps: count per second), and the horizontal axis shows the retention time (min); (b) Principal component analysis for metabolites identified in three different tissues of black tiger fruit viz. KP (peel), KF (pulp), and KD (seed).

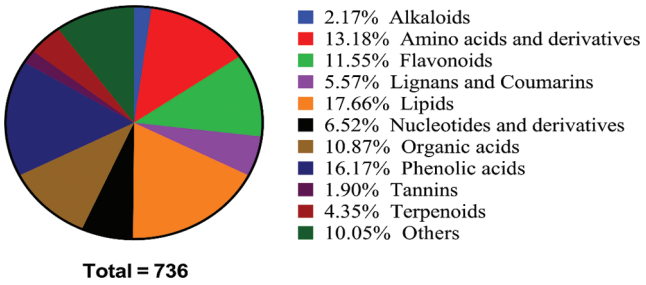

FIGURE 3. Pie chart representing the identified 736 metabolites and the corresponding major classes.

kadcoccinic acid G, delphinidin-3-O-(2”-O-xylosyl)rutinoside, cyanidin-3-O-(2”-O-glucosyl)rutinoside, cyanidin-3-O-rutinoside (keracyanin), kadcotrione C, cyanidin-3-O-glucoside (kuromanin), kadcoccitone C, lariciresinol-4’-O-glucoside, and rosmarinic acid-3’-O-glucoside showed up-accumulation in the pulp as compared to the seed (Fig. 7b).

Comparison of seed and peel (KP *vs.* KD) metabolome resulted in the identification of 533 DAMs, with 144 showing up-accumulation in the seed while 389 showed up-accumulation in the peel tissues (Tab. S4). The accumulation level of the identified DAMs between peel and seed has been presented in Fig. 8a. Pregomisin, kadangustin G, kadsuralignan G, kadangustin F, kadusurain C, kadsuralignan J, kadcoccilactone A, kadangustin I, kadsuralignan H, and acetylepigomisin R were among the up-accumulated metabolites in the seed (Fig. 8b). Epicatechin, 4-aminobenzoic acid, cyanidin-3-O-(2”-O-glucosyl) rutinoside, delphinidin-3-O-glucoside (mirtillin), cyanidin-3-O-rutinoside (keracyanin), quercetin-3-O-rutinoside (rutin), rosmarinic acid-3’-O-glucoside, lariciresinol-4’-O-glucoside, delphinidin-3-O-(2”-O-xylosyl) rutinoside and cyanidin-3-O-glucoside (kuromanin) showed up-accumulation in the peel compared to the seed (Fig. 8b).

Above mentioned metabolome comparisons suggested that peel tissues of black tiger fruit have more diverse and concentrated metabolites, particularly flavonoids compared to the pulp and seed. On the other hand, the seed also contains elevated amounts of lignans and coumarins.

Discussion

Metabolites are naturally occurring organic compounds present in living organisms, with the most common being flavonoids, amino acids, alkaloids, and lipids (Erb and Kliebenstein, 2020). In this study, we explored the metabolome of black tiger (*Kadsura coccinea* (Lem.)) fruit parts viz., peel, pulp, and seed using the widely-targeted metabolomics approach. Widely-targetted metabolomics provides an inclusive platform for identifying and further exploiting diverse metabolomes (Chen *et al.*, 2013; Sawada *et al.*, 2009). The study aimed to provide a comprehensive insight into the differential metabolome of different fruit parts of black tiger fruit, which is used in traditional Chinese medicine due to its antioxidant, anti-tumor, anti-HIV anti-lipid peroxidative, cytotoxic, and anti-hepatitis properties (Sritalahareuthai *et al.*, 2020a; Woo *et al.*, 2020).

The metabolome landscape of black tiger fruit revealed an elevated concentration of flavonoids, phenolic acids, terpenoids, and tannins in the peel than pulp and seed. However, lignans and coumarins showed significantly higher accumulation in the seed. Previous reports have also reported the identification of flavonoids (Sritalahareuthai *et al.*, 2020a), phenolic acids (Sun *et al.*, 2009), and lignans (Li *et al.*, 2006) from different tissues of the black tiger plant. Moreover, *K. coccinea* was shown to contain gallic acid (phenolic acid) (Sun *et al.*, 2011), with a strong DPPH-radical scavenging activity. The pulp showed a high abundance of flavonoids and lipids, and the most noticeable, with known beneficial effects on human health, are rutinoside (Matsumoto *et al.*, 2001; Olthof *et al.*, 2003), γ-linolenic acid (Fan and Chapkin, 1998), α-linolenic acid (Burdge, 2006), lysoPE 16:0 (Ren *et al.*, 2018), lysoPC 18:2

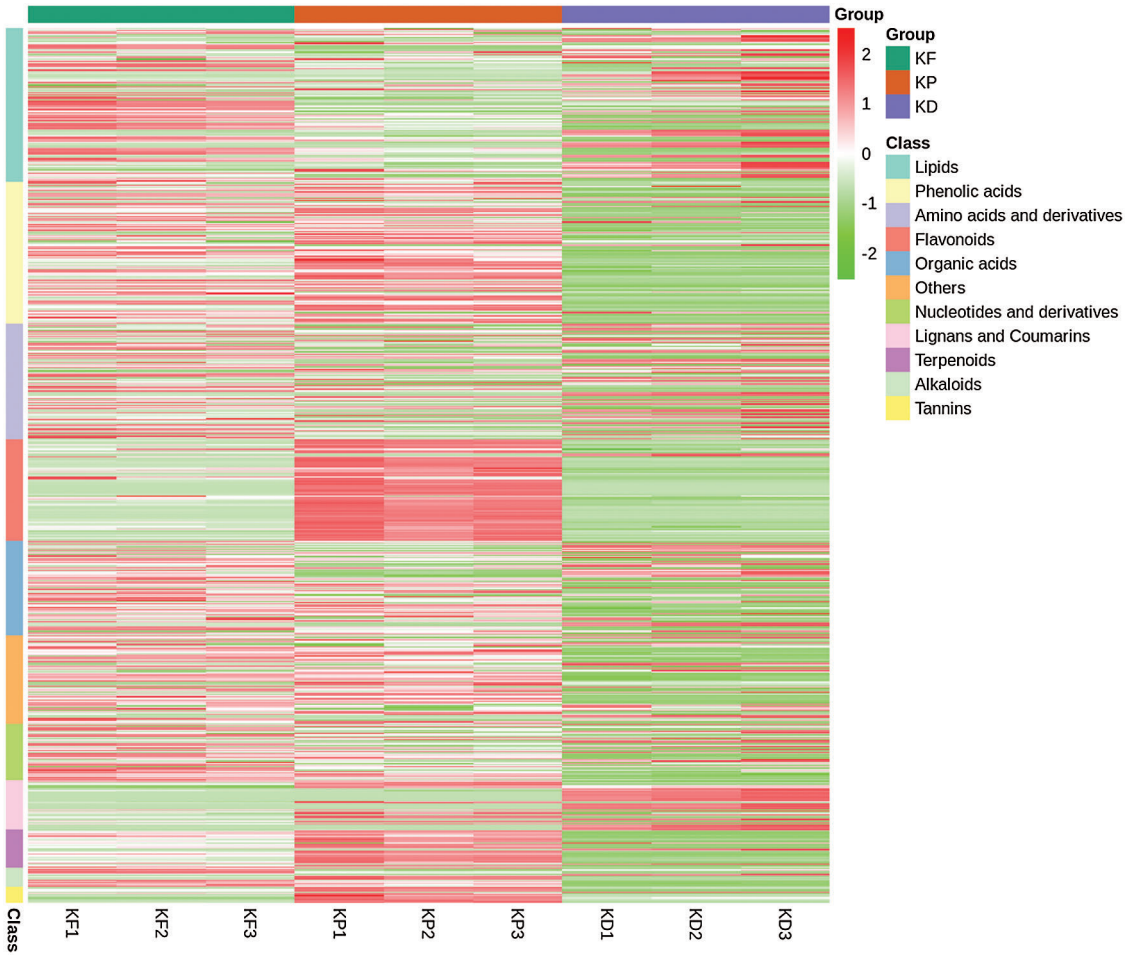

FIGURE 4. Heatmap representing the accumulation (ion intensity) of metabolites in three tissues KP (peel), KF (pulp), and KD (seed).

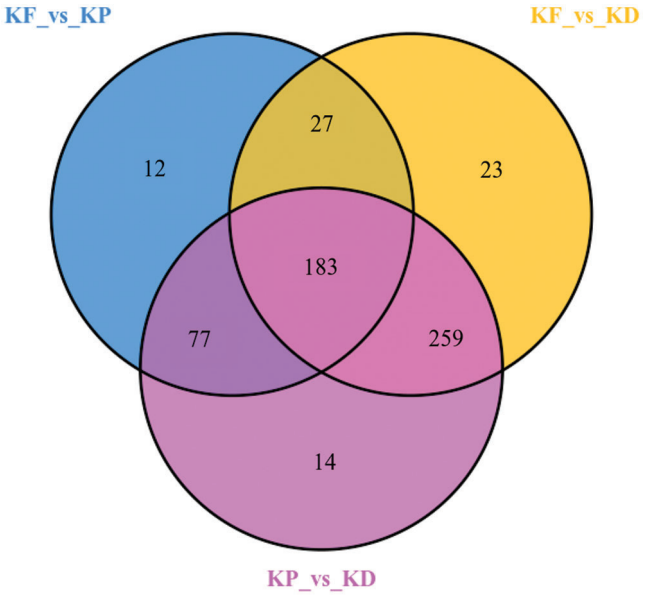

FIGURE 5. Venn diagram representing differentially accumulating metabolites (DAMs) between different tissues of the black tiger: peel (KP), pulp (KF) and seed (KP).

(2n isomer), stearic acid (Bonanome and Grundy, 1988), and lysoPC 18:2 (Dong *et al.*, 2010). Similarly, the peel showed an abundance of flavonoids. Cyanidin-3-O-glucoside, also known as "kuromanin" is responsible for red hue in different fruits (Olivas-Aguirre *et al.*, 2016) and is also known for its antioxidant and anti-tumor characteristics (Sun *et al.*, 2012). Nasser *et al.* (2019) reported neuroprotective effects of kuromanin chloride (Cyanidin-3-O-glucoside) against neurodegenerative diseases. A recent report by Sritalahareuthai *et al.* (2020b) emphasized the abundance of flavonoids in *K. coccinea* compared to other *Kadsura* species. Isorhamnetin-3-O-rutinoside (Narcissin) has been recently reported to inhibit COVID-19 virus main protease (Owis *et al.*, 2020). Delphinidin-3-O-(2''-O-xylosyl) rutinoside was also identified in the peel, which is an important flavonoid in the biosynthesis of purple to blue color in plants (Xu *et al.*, 2018). The presence of delphinidin-3-O-(2''-O-xylosyl) rutinoside and cyanidin-3-O-glucoside and their higher accumulation in peel tissues are predicted to confer the peculiar red peel color of black tiger fruit. Anthocyanidins are water-soluble pigmented compounds widely distributed in blue to purplish fruits (Sritalahareuthai *et al.*, 2020b), with cyanidin and delphinidin as the most abundant anthocyanidins (Dini *et al.*, 2019). Beyond pigmentation, anthocyanins also play a critical role as therapeutic agents for Central Nervous System (Cásedas *et al.*, 2020). Furthermore, we also identified gallocatechin, which has been previously reported in pomegranate (Plumb *et al.*, 2002), guava (Matsuo *et al.*, 1994), and tea (Ikeda *et al.*, 2003). Gallocatechin is an important flavonoid and displays a

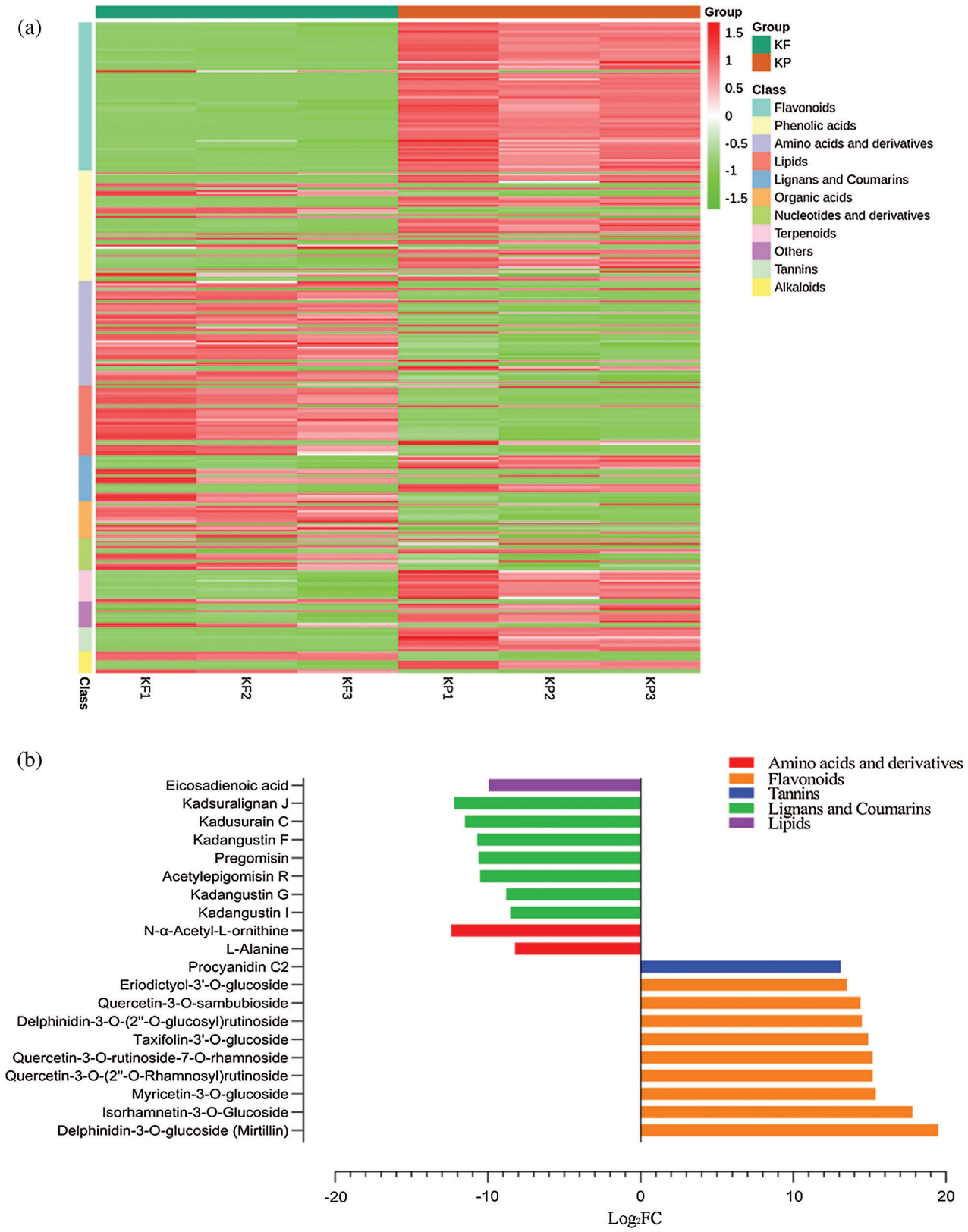

FIGURE 6. Identification of differentially accumulated metabolites (DAMs) between peel (KP) and pulp (KF), KF *vs.* KP.
(a) Heatmap representing accumulation profile of DAMs in peel and pulp tissues. (b) Top 20 metabolites differentially accumulated between KP and KF, where the x-axis represents $\log_2$FC of ion intensity.

cardiovascular protective effect (Hertog *et al.*, 1993; Plumb *et al.*, 2002).

In the seed, an abundance of lipids and lignans was observed. Previous reports suggested the significance of lipid and lignan compositions in the black tiger plant (Gao *et al.*, 2008a; Li *et al.*, 2006; Mulyaningsih *et al.*, 2010; Shao *et al.*, 2020). Seed and peel of black tiger fruit are generally considered biowaste; however, the abundance of bioactive

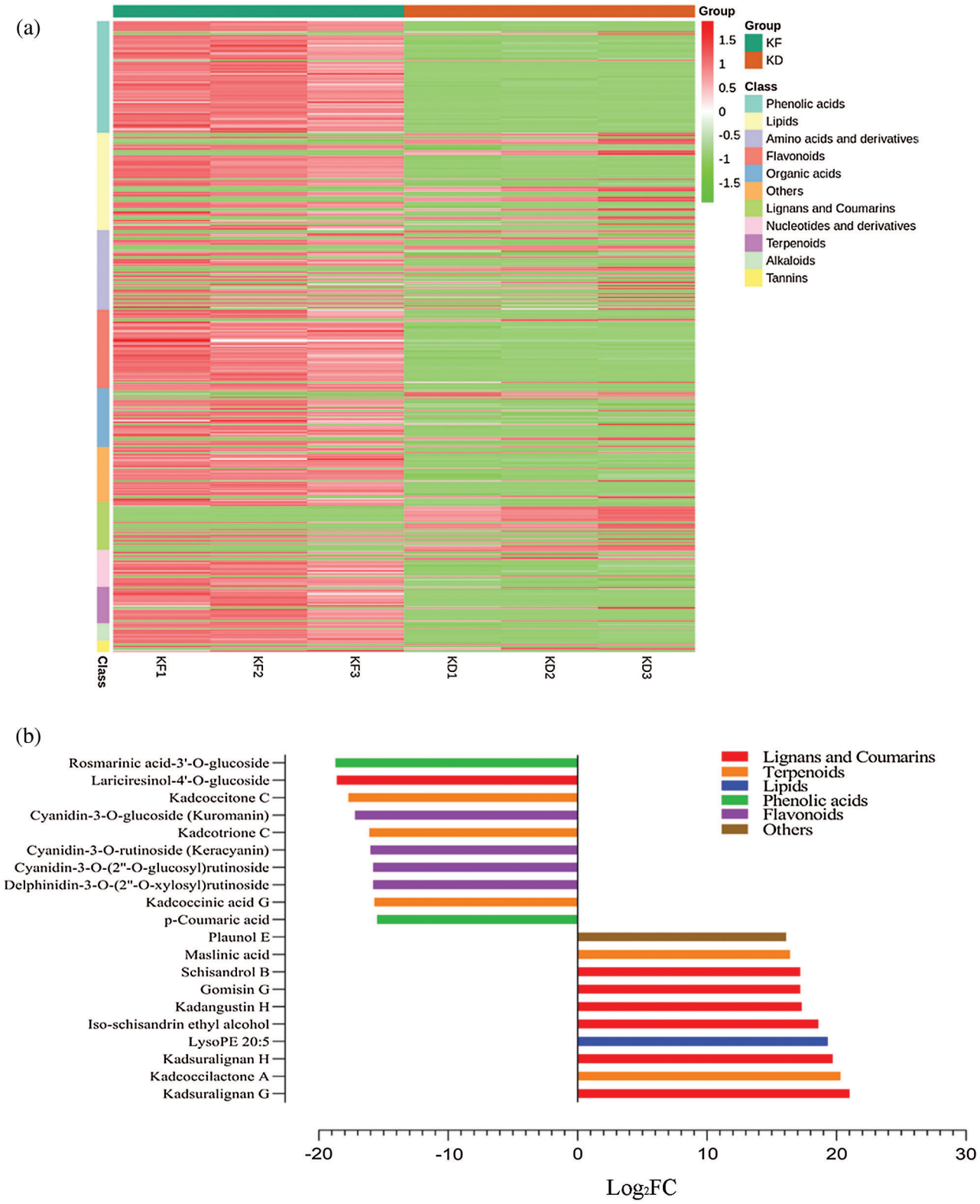

FIGURE 7. Identification of differentially accumulated metabolites (DAMs) between the seed (KD) and pulp (KF), KF *vs.* KD. (a) Heatmap representing accumulation profile of the DAMs in seed and pulp tissues. (b) Top 20 metabolites differentially accumulated between KD and KF, where the x-axis represents $\log_2$FC of ion intensity.

compounds in both tissues, as disclosed in this study, suggests possible valorization of these fruit parts. The most prominent lignans found in the seed were kadangustin E, pregomisin, kadangustin G, kadsuralignan G, kadangustin F, kadangustin D, kadusurain C, and kadsuralignan J. Previously published statistics by Liu *et al.* (2019) on comparative authentication of *Kadsura* crude drug suggested identification of kadangustin L and kadangustin E in *K. coccinea*. Gao *et al.* (2012) emphasized lignans and triterpenoids as principal bioactive compounds present in

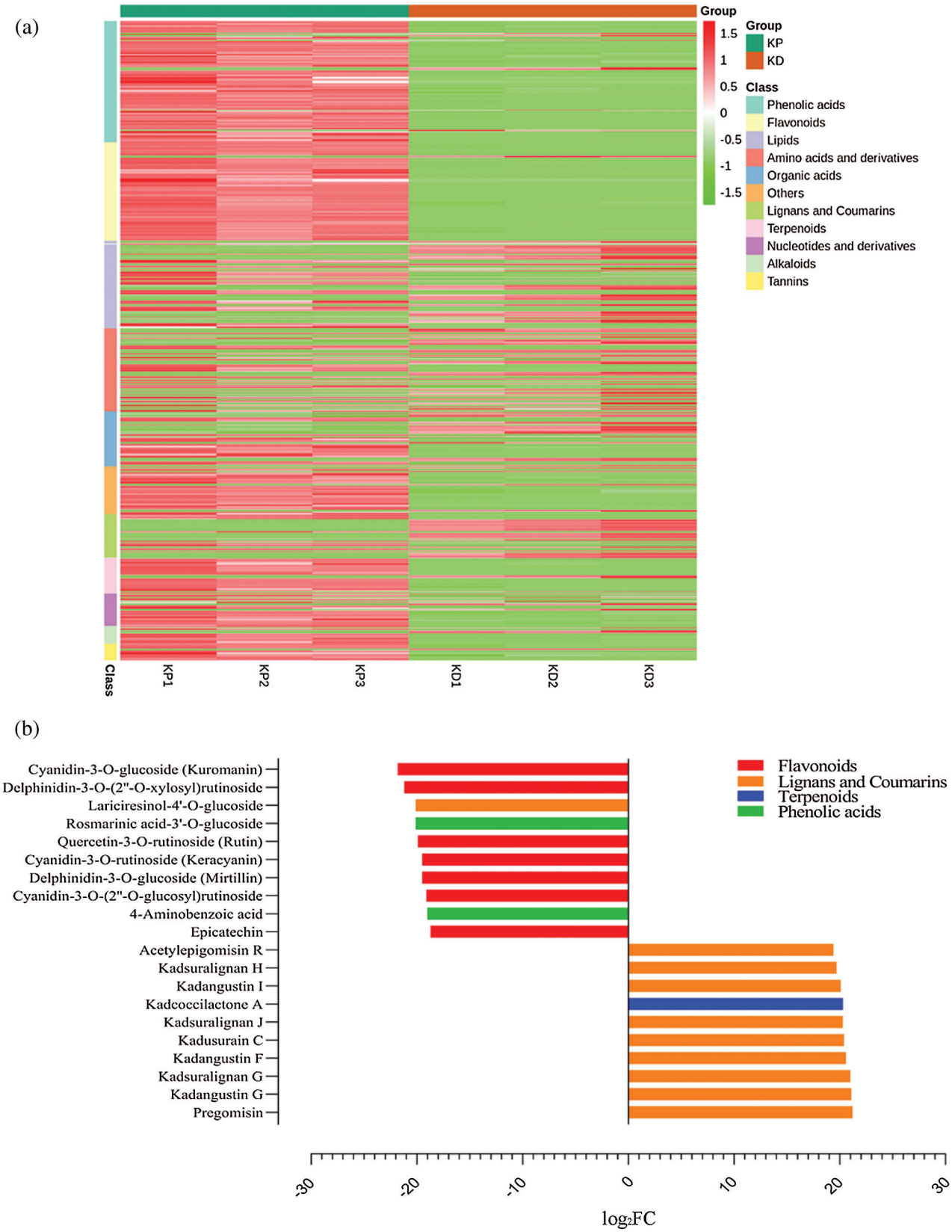

FIGURE 8. Identification of differentially accumulated metabolites (DAMs) between the seed (KD) and peel (KP), KP *vs.* KD. (a) Heatmap representing the metabolite accumulation levels of the DAMs in seed and peel tissues. (b) Top 20 metabolites differentially accumulated between KD and KP, where the x-axis represents $\log_2$FC of ion intensity.

K. coccinea with significant bioactivities related to anti-HIV, immunodeficiency, cytotoxicity, and antiproliferative effects. *Kadsura* genus is a rich source of lignans. Previously, reports highlighted an abundance of lignans in *K. angustifolia* (Gao *et al.*, 2008b; Liu *et al.*, 2019), *K. philippinensis* (Shen *et al.*, 2009), *K. longipedunculata* and *K. heteroclite* (Liu *et al.*, 2019). In contrast with a previous report (Liu *et al.*, 2019) suggesting a low abundance of kadangustin E in the stem of

K. coccinea, our results suggest a significant abundance of kadangustin E in the seed. Pregomisin (Yadav *et al*., 2019), kadangustin G (Gao *et al*., 2008b), kadsuralignan G (Goh *et al*., 2013), and kadsuralignan J (Liu *et al*., 2018b) have also been reported for their significant effects on human health and used in traditional medicine. Plant lipids are an excellent dietary source for human consumption (Ursin, 2003). Both pulp and seed tissues showed strong accumulation of linoleic acid, lysoPC 18:2, lysoPC 18:2(2n isomer), γ-linolenic acid, α-linolenic acid, and stearic acid.

Conclusions

Our study clarified the metabolome landscapes of the fruit peel, seed, and pulp in *K. coccinea*. Comparative metabolome analysis suggests that the peel and seed tissues of *K. coccinea* are enriched in bioactive secondary metabolites, especially flavonoids and lignans, and can be further valorized as human dietary sources or raw materials in the pharmaceutical industry. Furthermore, a multi-omics approach can decipher the biosynthesis pathways for identified key metabolites to improve their bioavailability. Quantification and biological activities of the identified metabolites can be resourceful for future studies.

Availability of Data and Materials: All data generated or analyzed during this study are included in this published article (and its supplementary information files).

Author Contributions: JG and KX conceived and designed the study; JG, WZ, and WL collected the samples and performed the experiments. JG analyzed the data and drafted the manuscript. KX provided financial support, supervised the study, and revised the first drafts of the manuscript. All authors have read and approved the final version of this manuscript.

Supplementary Material: The supplementary material is available online at DOI: 10.32604/biocell.2022.016253.

Ethics Approval: Not applicable.

Funding Statement: This work was funded by the Key Project of Science and Technology Program of Guizhou Province: Poverty Alleviation Model and Technology demonstration for Ecoindustries Derivated from the karst desertification control (No. 5411 2017 Qiankehe Pingtai Rencai), the National Key Research and Development Program during the 13th Five-Year Plan Period of China [No. 2016YFC0502601] and the Guizhou Province Science and Technology Plan Project "Guizhou medicinal and food dual-purpose fruit cold rice ball high-quality cultivation and product development (Qian Science and Technology Cooperation Support [2016] No. 2627).

Conflicts of Interest: The authors declare that they have no conflicts of interest to report regarding the present study.

References

Bonanome A, Grundy SM (1988). Effect of dietary stearic acid on plasma cholesterol and lipoprotein levels. *New England Journal of Medicine* **318**: 1244–1248.

Burdge G (2006). Metabolism of α-linolenic acid in humans. *Prostaglandins, Leukotrienes and Essential Fatty Acids* **75**: 161–168.

Cao L, Shehla N, Tasneem S, Cao M, Sheng W, Jian Y, Li B, Peng C, Choudhary MI, Atta-ur-Rahman, Liao DF, Wang W (2019). New cadinane sesquiterpenes from the stems of *Kadsura heteroclita*. *Molecules* **24**: 1664.

Cásedas G, Les F, López V (2020). Anthocyanins: plant pigments, food ingredients or therapeutic agents for the CNS? A mini-review focused on clinical trials. *Current Pharmaceutical Design* **26**: 1790–1798.

Chen W, Gong L, Guo Z, Wang W, Zhang H, Liu X, Yu S, Xiong L, Luo J (2013). A novel integrated method for large-scale detection, identification, and quantification of widely targeted metabolites: application in the study of rice metabolomics. *Molecular Plant* **6**: 1769–1780.

Deng G, Sheng O, Bi FC, Li CY, Dou TX, Dong T, Yang QS, Gao HJ, Liu J, Zhong XH (2020). Metabolic profiling in banana pseudo-stem reveals a diverse set of bioactive compounds with potential nutritional and industrial applications. *Phyton* **89**: 1101–1130.

Dini C, Zaro MJ, Viña SZ (2019). Bioactivity and functionality of anthocyanins: a review. *Current Bioactive Compounds* **15**: 507–523.

Dong J, Cai X, Zhao L, Xue X, Zou L, Zhang X, Liang X (2010). Lysophosphatidylcholine profiling of plasma: Discrimination of isomers and discovery of lung cancer biomarkers. *Metabolomics* **6**: 478–488.

Dossa K, Zhou R, Li DH, Liu AL, Qin L, Marie AM, Su RQ, Zhang YJ, Wang JQ, Gao Y, Zhang XR, You J (2020). A novel motif in the 5'-UTR of an orphan gene 'Big Root Biomass' modulates root biomass in sesame. *Plant Biotechnology Journal* **19**: 1065–1079.

El-Ishaq A, Obirinakem S (2015). Effect of temperature and storage on vitamin C content in fruits juice. *International Journal of Chemical and Biomolecular Science* **1**: 17–21.

Erb M, Kliebenstein DJ (2020). Plant secondary metabolites as defenses, regulators, and primary metabolites: the blurred functional trichotomy. *Plant Physiology* **184**: 39–52.

Fan YY, Chapkin RS (1998). Importance of dietary γ-linolenic acid in human health and nutrition. *Journal of Nutrition* **128**: 1411–1414.

Fiehn O, Wohlgemuth G, Scholz M, Kind T, Lee DY, Lu Y, Moon S, Nikolau B (2008). Quality control for plant metabolomics: reporting MSI-compliant studies. *Plant Journal* **53**: 691–704.

Gao XM, Pu JX, Huang SX, Lu Y, Lou LG, Li RT, Xiao WL, Chang Y, Sun HD (2008a). Kadcoccilactones A–J, triterpenoids from *Kadsura coccinea*. *Journal of Natural Products* **71**: 1182–1188.

Gao XM, Pu JX, Huang SX, Yang LM, Huang H, Xiao WL, Zheng YT, Sun HD (2008b). Lignans from *Kadsura angustifolia*. *Journal of Natural Products* **71**: 558–563.

Gao XM, Pu JX, Zhao Y, Yang LB, Sun HD (2012). Lignans from *Kadsura angustifolia* and *Kadsura coccinea*. *Journal of Asian Natural Products Research* **14**: 129–134.

Goh MJ, Lee HK, Cheng L, Kong DY, Yeon JH, He QQ, Cho JC, Na YJ (2013). Depigmentation effect of kadsuralignan f on melan-a murine melanocytes and human skin equivalents. *International Journal of Molecular Sciences* **14**: 1655–1666.

Hao J, Zhu H, Liu S, Li H (2014). Characterization of anthocyanins in fruit of *Kadsura coccinea* (Lem.) AC Smith by UPLC/Q-TOF-MS analysis and evaluation of stability of the major anthocyanins. *Food Analytical Methods* **7**: 1312–1322.

Hertog MG, Feskens EJ, Kromhout D, Hollman P, Katan M (1993). Dietary antioxidant flavonoids and risk of coronary heart disease: The Zutphen Elderly Study. *Lancet* **342**: 1007–1011.

Hu ZX, Shi YM, Wang WG, Tang JW, Zhou M, Du X, Zhang YH, Pu JX, Sun HD (2016). Structural characterization of kadcoccinin A: A sesquiterpenoid with a tricyclo [4.4. 0. 03, 10] decane scaffold from *Kadsura coccinea*. *Organic Letters* **18**: 2284–2287.

Ikeda I, Kobayashi M, Hamada T, Tsuda K, Goto H, Imaizumi K, Nozawa A, Sugimoto A, Kakuda T (2003). Heat-epimerized tea catechins rich in gallocatechin gallate and catechin gallate are more effective to inhibit cholesterol absorption than tea catechins rich in epigallocatechin gallate and epicatechin gallate. *Journal of Agricultural and Food Chemistry* **51**: 7303–7307.

Kuo YH, Wu MD, Huang RL, Kuo LMY, Hsu YW, Liaw CC, Hung CC, Shen YC, Ong CW (2005). Antihepatitis activity (anti-HBsAg and anti-HBeAg) of C19 homolignans and six novel C18 dibenzocyclooctadiene lignans from *Kadsura japonica*. *Planta Medica* **71**: 646–653.

Li HR, Feng YL, Yang ZG, Wang J, Daikonya A, Kitanaka S, Xu LZ, Yang SL (2006). New lignans from *Kadsura coccinea* and their nitric oxide inhibitory activities. *Chemical and Pharmaceutical Bulletin* **54**: 1022–1025.

Li H, Wang L, Yang Z, Kitanaka S (2007). Kadsuralignans H–K from *Kadsura coccinea* and their nitric oxide production inhibitory effects. *Journal of Natural Products* **70**: 1999–2002.

Liu J, Pandey P, Wang X, Qi X, Chen J, Sun H, Zhang P, Ding Y, Ferreira D, Doerksen RJ (2018a). Hepatoprotective dibenzocyclooctadiene and tetrahydrobenzocyclooctabenzofuranone lignans from *Kadsura longipedunculata*. *Journal of Natural Products* **81**: 846–857.

Liu J, Qi Y, Lai H, Zhang J, Jia X, Liu H, Zhang B, Xiao P (2014). Genus *Kadsura*, a good source with considerable characteristic chemical constituents and potential bioactivities. *Phytomedicine* **21**: 1092–1097.

Liu J, Wei X, Zhang X, Qi Y, Zhang B, Liu H, Xiao P (2019). A comprehensive comparative study for the authentication of the *Kadsura* crude drug. *Frontiers in Pharmacology* **9**: 1576.

Liu Y, Yang Y, Tasneem S, Hussain N, Daniyal M, Yuan H, Xie Q, Liu B, Sun J, Jian Y (2018b). Lignans from Tujia ethnomedicine Heilaohu: chemical characterization and evaluation of their cytotoxicity and antioxidant activities. *Molecules* **23**: 2147.

Matsumoto H, Inaba H, Kishi M, Tominaga S, Hirayama M, Tsuda T (2001). Orally administered delphinidin 3-rutinoside and cyanidin 3-rutinoside are directly absorbed in rats and humans and appear in the blood as the intact forms. *Journal of Agricultural and Food Chemistry* **49**: 1546–1551.

Matsuo T, Hanamure N, Shimoi K, Nakamura Y, Tomita I (1994). Identification of (+)-gallocatechin as a bio-antimutagenic compound in *Psidium guava* leaves. *Phytochemistry* **36**: 1027–1029.

Mulyaningsih S, Youns M, El-Readi MZ, Ashour ML, Nibret E, Sporer F, Herrmann F, Reichling J, Wink M (2010). Biological activity of the essential oil of *Kadsura longipedunculata* (Schisandraceae) and its major components. *Journal of Pharmacy and Pharmacology* **62**: 1037–1044.

Nasser H, Kader HM, Al Mughairbi F (2019). Neuroprotective effects of kuromanin chloride (anthocyanin) against glutamatergic excitotoxicity in neuroblastoma cells. *Frontiers in Human Neuroscience* **13**. DOI 10.3389/conf.fnhum.2019.3229.00035. https://www.frontiersin.org/10.3389%2fconf.fnhum.2019.229.00035/event_abstract.

Olivas-Aguirre FJ, Rodrigo-García J, Martínez-Ruiz NdR, Cárdenas-Robles AI, Mendoza-Díaz SO, Alvarez-Parrilla E, González-Aguilar GA, De la Rosa LA, Ramos-Jiménez A, Wall-Medrano A (2016). Cyanidin-3-O-glucoside: Physical-chemistry, foodomics and health effects. *Molecules* **21**: 1264.

Olthof MR, Hollman PC, Buijsman MN, Van Amelsvoort JM, Katan MB (2003). Chlorogenic acid, quercetin-3-rutinoside and black tea phenols are extensively metabolized in humans. *Journal of Nutrition* **133**: 1806–1814.

Owis AI, El-Hawary MS, El Amir D, Aly OM, Abdelmohsen UR, Kamel MS (2020). Molecular docking reveals the potential of *Salvadora persica* flavonoids to inhibit COVID-19 virus main protease. *RSC Advances* **10**: 19570–19575.

Plumb G, De Pascual-Teresa S, Santos-Buelga C, Rivas-Gonzalo JC, Williamson G (2002). Antioxidant properties of gallocatechin and prodelphinidins from pomegranate peel. *Redox Report* **7**: 41–46.

Ren C, Liu J, Zhou J, Liang H, Wang Y, Sun Y, Ma B, Yin Y (2018). Lipidomic analysis of serum samples from migraine patients. *Lipids in Health and Disease* **17**: 22.

Sawada Y, Akiyama K, Sakata A, Kuwahara A, Otsuki H, Sakurai T, Saito K, Hirai MY (2009). Widely targeted metabolomics based on large-scale MS/MS data for elucidating metabolite accumulation patterns in plants. *Plant and Cell Physiology* **50**: 37–47.

Shao SY, Qi XZ, Sun H, Li S (2020). Hepatoprotective lignans and triterpenoids from the roots of *Kadsura longipedunculata*. *Fitoterapia* **142**: 104487.

Shen YC, Lin YC, Cheng YB, Chiang MY, Liou SS, Khalil AT (2009). Dibenzocyclooctadiene lignans from *Kadsura philippinensis*. *Phytochemistry* **70**: 114–120.

Sritalahareuthai V, Aursalung A, On-Nom N, Temviriyanukul P, Charoenkiatkul S, Suttisansanee U (2020a). Nutritional composition of conserved *Kadsura* spp. plants in Northern Thailand. *Heliyon* **6**: e04451.

Sritalahareuthai V, Temviriyanukul P, On-Nom N, Charoenkiatkul S, Suttisansanee U (2020b). Phenolic profiles, antioxidant, and inhibitory activities of *Kadsura heteroclita* (Roxb.) Craib and *Kadsura coccinea* (Lem.) A.C. Sm. *Foods* **9**: 1222.

Sun C, Zheng Y, Chen Q, Tang X, Jiang M, Zhang J, Li X, Chen K (2012). Purification and anti-tumour activity of cyanidin-3-O-glucoside from Chinese bayberry fruit. *Food Chemistry* **131**: 1287–1294.

Sun J, Jiang Y, Amin I, Li Z, Prasad K, Duan X, Yang B, Xu L (2011). An exotic fruit with high nutritional value: *Kadsura coccinea* fruit. *International Food Research Journal* **18**: 651–657.

Sun J, Yao J, Huang S, Long X, Wang J, García-García E (2009). Antioxidant activity of polyphenol and anthocyanin extracts from fruits of *Kadsura coccinea* (Lem.) A.C. Smith. *Food Chemistry* **117**: 276–281.

Ursin VM (2003). Modification of plant lipids for human health: development of functional land-based omega-3 fatty acids. *Journal of Nutrition* **133**: 4271–4274.

Wang J, Guo D, Han D, Pan X, Li J (2020a). A comprehensive insight into the metabolic landscape of fruit pulp, peel, and seed in two longan (*Dimocarpus longan* Lour.) varieties. *International Journal of Food Properties* **23**: 1527–1539.

Wang M, Jiang S, Yuan H, Zafar S, Hussain N, Jian Y, Li B, Gong L, Peng C, Liu C (2020b). A review of the phytochemistry and pharmacology of *Kadsura heteroclita*, an important plant in

Tujia ethnomedicine. *Journal of Ethnopharmacology* **268**: 113567.

Woo MH, Nguyen DH, Choi JS, Park SE, Thuong PT, Min BS, Le DD (2020). Chemical constituents from the roots of *Kadsura coccinea* with their protein tyrosine phosphatase 1B and acetylcholinesterase inhibitory activities. *Archives of Pharmacal Research* **43**: 204–213.

Xu L, Xu Z, Wang X, Wang B, Liao X (2020). The application of pseudotargeted metabolomics method for fruit juices discrimination. *Food Chemistry* **316**: 126278.

Xu W, Luo G, Yu F, Jia Q, Zheng Y, Bi X, Lei J (2018). Characterization of anthocyanins in the hybrid progenies derived from *Iris dichotoma* and I. domestica by HPLC-DAD-ESI/MS analysis. *Phytochemistry* **150**: 60–74.

Yadav M, Mohanta R, Yadav K (2019). Ethno pharmacological approach of anti-obesity medicinal plants: A review. *Journal of Pharmacognosy and Phytochemistry* **8**: 1793–1798.

Yang X, Xia X, Zhang Z, Nong B, Zeng Y, Wu Y, Xiong F, Zhang Y, Liang H, Pan Y, Dai (2019a). Identification of anthocyanin biosynthesis genes in rice pericarp using PCAMP. *Plant Biotechnology Journal* **17**: 1700–1702.

Yang YP, Hussain N, Zhang L, Jia YZ, Jian YQ, Li B, Choudhary MI, Rahman AU, Wang W (2020). *Kadsura coccinea*: A rich source of structurally diverse and biologically important compounds. *Chinese Herbal Medicines* **12**: 214–223.

Yang Y, Liu Y, Daniyal M, Yu H, Xie Q, Li B, Jian Y, Man R, Wang S, Zhou X (2019b). New lignans from roots of *Kadsura coccinea*. *Fitoterapia* **139**: 104368.

Supplementary Materials

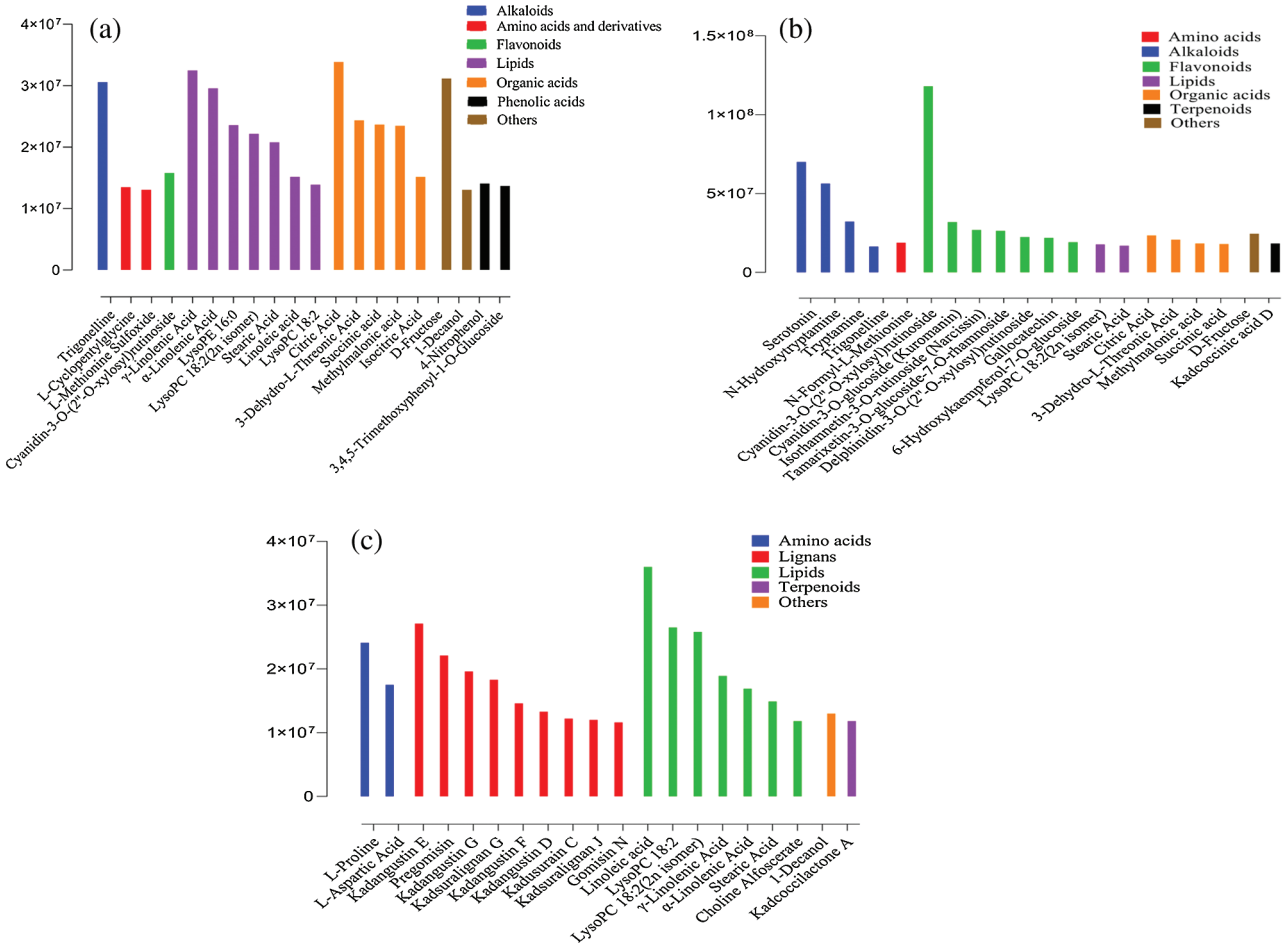

FIGURE S1. Top 20 metabolites and their ion intensity in respective tissues.
(a) Top 20 metabolites and their corresponding classification in pulp (KF), (b) Top 20 metabolites and their corresponding classification in peel (KP), (c) Top 20 metabolites and their corresponding classification in seed (KD) of the black tiger.

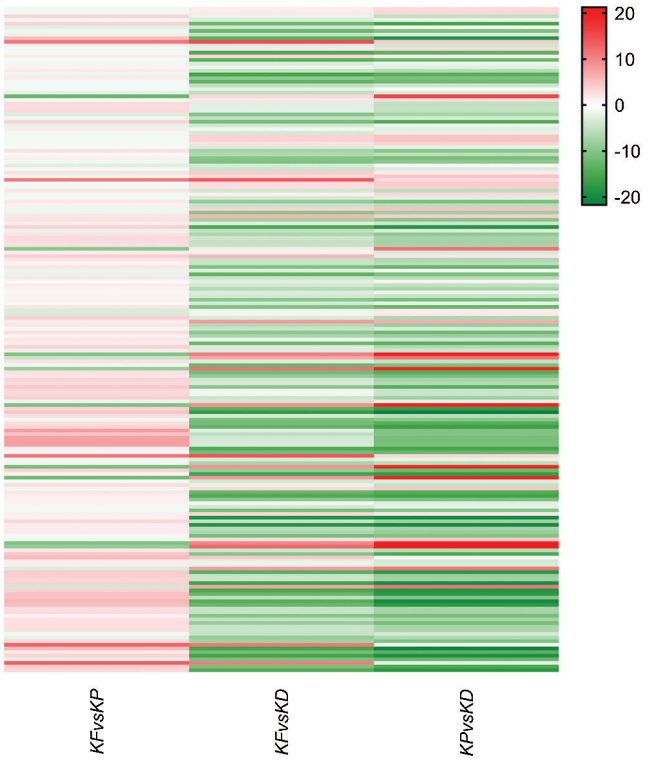

FIGURE S2. Heatmap representing the differential accumulation of metabolites in three group comparisons KF *vs.* KP, KF *vs.* KD, and KP *vs.* KD, where KF, KP, and KD correspond to black tiger fruit pulp, peel, and seed tissues, respectively.

TABLE S1

Metabolic landscape of black tiger fruit and respective tissues, i.e., peel, pulp, and seed

TABLE S2

Differentially expressed metabolites between pulp and peel tissues (KF *vs.* KP) of black tiger fruit.

TABLE S3

Differentially expressed metabolites between pulp and seed tissues (KF *vs.* KD) of black tiger fruit.

TABLE S4

Differentially expressed metabolites between peel and seed tissues (KP *vs.* KD) of black tiger fruit.

TABLE S5

Conserved differentially expressed metabolites between different tissues of black tiger fruit.